ACS APPLIED MATERIALS & INTERFACES

Article

Controlling the Uptake and Regulating the Release of Nitric Oxide in Microporous Solids

Rana R. Haikal, Carol Hua, John J. Perry IV, Daniel O'Nolan, Imran Syed, Amrit Kumar, Adrian H. Chester, Michael J. Zaworotko, Magdi Habeeb Yacoub, and Mohamed H. Alkordi

ACS Appl. Mater. Interfaces, **Just Accepted Manuscript** • DOI: 10.1021/acsami.7b15095 • Publication Date (Web): 28 Nov 2017

Just Accepted

ACS Publications

ACS Applied Materials & Interfaces is published by the American Chemical Society.
1155 Sixteenth Street N.W., Washington, DC 20036

Controlling the Uptake and Regulating the Release of Nitric Oxide in Microporous Solids

Rana R. Haikal,[a] Carol Hua,[b] John J. Perry IV,[b] Daniel O'Nolan,[b] Imran Syed, [b] Amrit Kumar, [b] Adrian H. Chester,[c] Michael J. Zaworotko,[b]* Magdi H. Yacoub,[c]* and Mohamed H. Alkordi[a]*

a Center for Materials Science, Zewail City of Science and Technology, Sheikh Zayed Dist., 12588, Giza, Egypt

b Bernal Institute, Department of Chemical Sciences, University of Limerick, Limerick V94 T9PX, Ireland

c Heart Science Centre, Imperial College, Harefield, Uxbridge UB9 6JH, United Kingdom

KEYWORDS: Nitric oxide sorption, microporous solids, acid-triggered release, porous-organic polymer, chemisorption.

ABSTRACT: Representative compounds from three classes of microporous solids, namely metal-organic frameworks (MOFs), hybrid ultramicroporous materials (HUMs) and porous-organic polymers (POPs), were investigated for their nitric oxide gas uptake and release behavior. Low pressure sorption studies indicated strong chemisorption of NO on the free amine groups decorating the MOF UiO-66-NH_2 when compared to its non-amine functionalized parent. The HUMs demonstrated reversible physisorption within the low pressure regime but interestingly in one case there was evidence for chemisorption following pressurization with NO at 10 bar. Significant release of chemisorbed NO from the UiO-66-NH_2 and one of the HUMs was triggered by addition of acid to the medium, a pH change from 7.4 to 5.4 being sufficient to trigger NO release. An imidazole-based POP exhibited chemisorption of NO at high pressure wherein the ring basicity facilitated both NO uptake and spontaneous release upon contact with the aqueous release medium.

1. Introduction

Nitric oxide (NO) is a mediator of numerous biological processes which are fundamental to the regulation of the nervous, immune and cardiovascular systems. NO is released by the action of nitric oxide synthase enzymes on L-arginine.[1] As a key endogenously excreted signaling molecule, disruption to its synthesis or bioavailability is believed to underpin a range of cardiovascular diseases, and its implications in pulmonary arterial hypertension (PAH) are under active investigations.[2-3] As such, it is a target for pharmacological strategies that aim to replace or mimic the biological effects of nitric oxide as a treatment for diseases where NO impairment is a feature.[4] Towards this goal, materials capable of the targeted delivery of NO at controllable rates and quantities, with appropriate modes of triggered release are of great potential therapeutic value.[5] Moreover, due to the narrow therapeutic range as an inhaled therapy and the potential toxic effects of NO gas, its administration is generally restricted to clinical environments via the use of pressurized containers. Materials capable of storing and delivering therapeutic dosages of NO, that are both safe for transportation and require minimal precautions, are therefore of great potential clinical and commercial value.

Examples of NO carriers currently investigated include NONOates, [6-9] metal-exchanged zeolites,[10] and metal-organic frameworks (MOFs)[11] amongst others.[12-15] NONOates were among the first compounds to be studied for potential NO delivery,[6-9] and are molecular species capable of releasing chemically bound NO upon contact with water. Alternatively, microporous solid sorbents such as zeolites and MOFs [16] enable NO to be physisorbed or chemically fixed to the walls of the material. Some classes of microporous solids are of particular promise as they can be fine-tuned in order to optimize host-guest interactions.[17] It is therefore unsurprising that MOFs with high surface area, intricate pore systems, and facile decoration by several chemical functionalities [18-20] have been examined for their potential in NO sorption.[21-23] Another class of physisorbent materials is hybrid ultramicroporous materials (HUMs), which combine two features thought to enhance sorbent-sorbate interactions: strong electrostatics in the form of inorganic anions with electronegative atoms; ultramicropores (<0.7 nm) that provide a tailored fit for important sorbates. HUMs exhibit exceptional molecular recognition capabilities for certain gas molecules[17, 24-28] but are yet to be studied in the context of NO. Covalent porous-organic polymers (POPs)[29-30] are also candidates for NO uptake and release due to the wide spectrum of chemical functionalities that can be incorporated. [31-34] Herein, we present a comparative study with archetypal MOFs, HUMs, and POPs to investigate structure-function relationships in the context of NO sorption and release (**Fig. 1**). The low pressure (0 –1 atm) sorption properties of representative MOFs, HUMs, and POPs were measured along with their NO release in phosphate buffer saline (PBS) after NO loading at 10 bar. The compounds investigated include the prototypical (UiO-66)[35] and its amine-functionalized analog (UiO-66-NH_2),[18] three recently

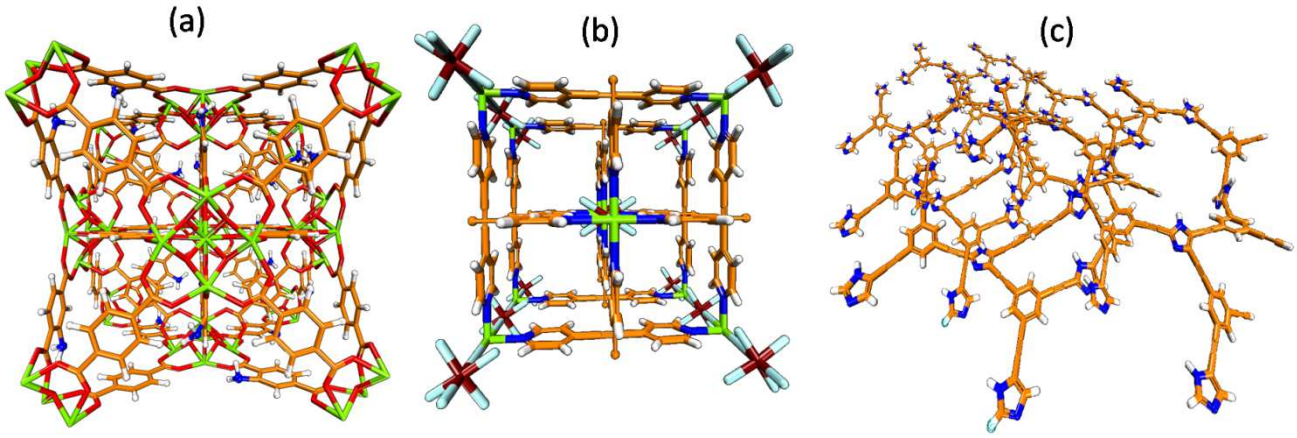

Figure 1. (a) Crystal structure ofUiO-66-NH_2(MOF), (b) crystal structure of TIFSIX-2-Cu-i (HUM), and (c) a geometrically optimized model for a tentative repeat unit in the imidazole-POP. C (orange), N (blue), O (red), H (white), Ti (deep red), F (light blue), Cu and Zr (green).

reported TIFSIX HUMs,[17] and an imidazole-based POP reported here for the first time. UiO-66-NH_2 was selected due to its high surface area, the presence of amine functionality capable of forming *N*-diazeniumdiolates with NO, and in contrast to many MOFs, its enhanced water stability.[36-37] The three HUMs represent an opportunity to explore the relative significance of NO-metal ion coordination versus potential strong physical interactions within the pores of the solids. Finally, the POP studied herein is a microporous solid wherein imidazole rings constitute an integral part of the framework, potentially leading to chemisorption of NO. Our investigation of the NO release profiles begin at neutral pH (PBS), before acid is added in a later stage of the release, allowing determination of acid-triggered release of NO, low pH having been reported to facilitate NO release from NONOates.

2. Results and Discussion

Established protocols for the synthesis and activation of Zr-carboxylate (UiO-66 and UiO-66-NH_2) MOFs were adopted.[38] Similarly, for synthesis of the three HUMs (TIFSIX-2-Cu-i, TIFSIX-4-Cu-i, and TIFSIX-3-Ni), previously published procedures were followed.[17, 39] The imidazole-POP was synthesized through the Sonogashira-Hagihara cross coupling reaction,[40] followed by guest exchange as described in the experimental section. The as-synthesized compounds were characterized using Fourier-transform infrared spectroscopy (FTIR), X-ray powder diffraction (PXRD) and N_2 or CO_2 sorption isotherms.

2.1 FTIR Spectroscopy

FTIR spectra were recorded for the studied compounds before, **Fig.2a**, and after NO loading at 10 bar, **Fig. 2b (Fig. S1-S5** for more details). The distinct changes in FTIR spectra between the activated compounds and after loading with NO are discussed below. Upon loading UiO-66-NH_2 with NO, two new peaks at 1294 and 1710 cm^{-1} appear, which can be assigned to reaction of the primary amine with two equivalents of NO to form the *N*-diazeniumdiolate species.[21] Additionally, a peak at 1429 cm^{-1}, attributed to a $\nu_{C\text{-}NH2}$ stretching mode coupled with $\nu_{C\text{-}C}$ ring modes,[41] disappeared upon loading with NO, further supporting that reaction of NO with the amine had occurred. For the HUMs, it is postulated that binding of the NO will occur through a phase change whereupon an open metal site is generated.[42] Generally, the coordination of NO to a transition metal will manifest itself in a stretching peak in the range of 1500-1900 cm^{-1}, depending on the metal involved and the linear or bent coordination mode of the NO molecule.[43] TIFSIX-2-Cu-i and TIFSIX-4-Cu-i both demonstrated similar changes in their FTIR spectra upon loading with NO, which is unsurprising given that they are isostructural and only vary in the ligand present. Upon loading with NO, peaks at 1403, 1292 and 929 cm^{-1} appeared for TIFSIX-4-Cu-i while peaks at 1484, 1288 and 998 cm^{-1} appeared for TIFSIX-2-Cu-i, (see SI for more details). These peaks may be attributed to interaction of NO with the frameworks. For a Cu(II)-NO adduct, a peak is expected between 1700-1850 cm^{-1}. The FTIR of the as-synthesized TIFSIX-2-Cu-i solid, (**Fig. S2**) demonstrated a strong peak at 1616 cm^{-1} which upon loading with NO is broadened and appeared as a shoulder on a stronger peak that appeared at 1630 cm^{-1}.[44] Upon loading TIFSIX-2-Cu-i with NO, a distinct color change from a light grey-green to green was observed, indicating coordination to the Cu ions and supporting a chemisorption process. Upon loading TIFSIX-3-Ni with NO, four peaks appeared in the FTIR spectrum at 1763, 1393, 1305 and 1252 cm^{-1}. It is known that SIFSIX-3-Ni, an analogue of TIFSIX-3-Ni, adsorbs a significant quantity of water upon exposure to the atmosphere[28] and that it undergoes a reversible phase change to a layered structure when subjected to differential vapor sorption (DVS) studies using water vapor.[45] Water has been shown to have a significant effect on the frequency of the NO stretch where the Fe(II)-NO adduct in MIL-101(Fe) was significantly red shifted from 1807 cm^{-1} under dry conditions to 1770 cm^{-1} in the presence of water.[46] It has previously been reported that the Ni(II)-NO adduct appears between 1843-1807 cm^{-1},[47] however with the likely presence of water within the framework, the peak at 1763 cm^{-1} may be assigned to formation of the Ni(II)-NO adduct. The FTIR for the imidazole-POP is shown in **Fig. 2.** That the desired POP has been prepared is supported by a detectable change in the $\nu_{C\equiv C}$ stretching frequency from 2108 cm^{-1} in triethynylbenzene to 2174 cm^{-1} in the imidazole-POP, indicating a terminal to internal alkyne transformation. Moreover, the transformation into internal alkyne was confirmed

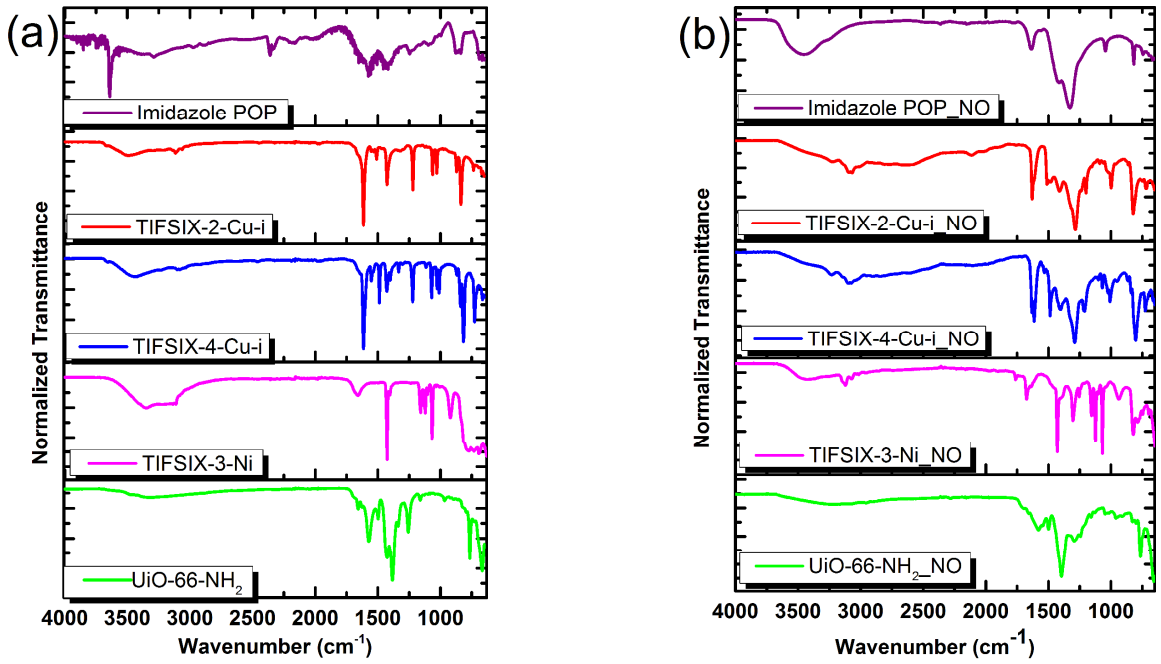

Figure 2. FTIR spectra for the (a) activated solids and (b) those after loading with NO.

by the strong attenuation to the terminal alkyne ν_{C-H} stretching frequency, where a strong peak was observed at 3274 cm^{-1} in the starting triethynylbenzene. A sharp, strong absorption peak observed at 3650 cm^{-1} in the imidazole-POP can potentially be ascribed to non-hydrogen bonded N-H stretching, expected for relatively displaced segments of the backbone in the microporous POP. After loading with NO (loading at 10 bar followed by pressure release to atmospheric pressure), dramatic changes to the FTIR spectrum were observed. A noticeable strong absorption at 1421 cm^{-1} was recorded and is in good agreement with that previously assigned to the –N=N–O group, [21] indicating immobilization of NO as *N*-diazeniumdiolate. Additionally, a broad peak was observed at 3500 cm^{-1}, and can be ascribed to hydrogen-bonded N-H stretching, potentially from the imidazole-*N*-diazeniumdiolate species.

2.2 Gas sorption isotherms

For UiO-66-NH_2 and imidazole-POP, it was difficult to fully regenerate the activated solid after the first NO sorption isotherm was conducted, due to pronounced desorption hysteresis indicating trapping or chemisorption of NO (**Fig. 3**). Notably, UiO-66-NH_2 demonstrated appreciable uptake of NO, with a steep rise at low pressures and noticeable desorption hysteresis. This is in contrast to the isotherm recorded for UiO-66, where a type-I isotherm was observed with minimal desorption hysteresis. This observation indicates chemisorption of the NO onto the amine functionalized MOF, and is in agreement with previous reports utilizing amine functionalized MOFs or those with open metal sites where NO can be anchored. The total uptake of NO by UiO-66-NH_2 at 760 torr was 160 cm^3/g. Using a formula unit of $ZrO_5C_8NH_5$ for guest-free UiO-66-NH_2, with a calculated molecular mass of 286.35 g/mol (giving rise to 3.5 mmol of the amine group per g of the material), and accordingly the calculated NO uptake assuming two NO molecules per amine functionality

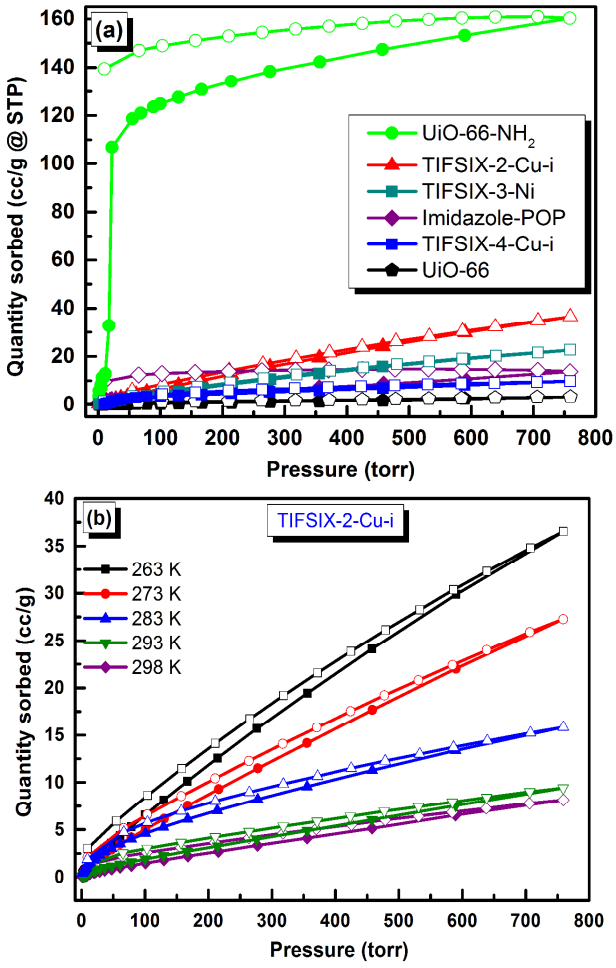

Figure 3.(a) NO sorption isotherms for the compounds studied herein and (b) the variable temperature sorption isotherms for TIFSIX-2-Cu-i. Adsorption (closed symbol) and desorption (open symbols).

was found to be 7 mmol/g. The adsorption isotherm of the UiO-66-NH_2 demonstrated an uptake of 7.1 mmol/g of NO, while upon conducting the desorption measurements the amount of trapped NO was 139 cm^3/g, equivalent to 6.2 mmol/g. Therefore, it can be asserted that NO chemisorption has occurred in UiO-66-NH_2 with up to 2 NO molecules per amine group. The NO sorption isotherms for the three HUMs demonstrated type-I isotherms, indicating reversible physisorption of NO within the pores of the compound at the pressure range of 0 to 1 bar of NO. The NO sorption isotherms collected for the TIFSIX-2-Cu-i (as a representative to HUMs) enabled calculating the isosteric heat of adsorption (Qst, **Fig. 4**) to be considerably high and within a range of 37~35 kJ/mol. The linear shape of the Qst plot over the entire uptake range indicated fairly homogenous adsorption sites for NO inside the TIFSIX-2-Cu-i. The NO isotherm for the imidazole-POP demonstrated a noticeable desorption hysteresis, indicating chemisorption of NO by the POP. The amount of trapped NO within the pores of the POP, as calculated from the last desorption point, was 0.4 mmol/g or 1.2 wt%. Notably, neither the HUMs nor the imidazole-POP saturate with NO at 1 bar in contrast to UiO-66-NH_2. Higher NO loadings are therefore attainable if the material is dosed at a higher NO pressure. The NO loading for the release study was conducted at 10 bar of NO in order to maximize the amount of NO that can be stored within the materials studied herein.

2.3 Other characterization techniques

The powder x-ray diffraction (PXRD) patterns for the three HUMs are provided in **SI** (**Fig. S7-S11**) and match those published previously. Similarly, the PXRD patterns for the two UiO-66 MOFs closely match those reported in the literature. Imidazole-POP was found to be amorphous, as commonly encountered in similar POPs. The composition of the imidazole-POP was therefore investigated using cross-polarization, magic angle spinning ^{13}C-solid state (^{13}C-CPMAS) NMR spectroscopy, **Fig.5**. The ^{13}C-CPMAS-NMR spectrum of the imidazole-POP indicates the presence of internal alkyne, two peaks at 80 and 90 ppm. The two different chemical shift values are indicative of two distinct environments for the internal alkyne carbons, and were assigned for the *sp* carbon atoms connected to the imidazole ring (80 ppm) and on the tritopic triethynylbenzene (90 ppm). The aromatic region of the spectrum displayed a relatively sharp peak at 122.5 ppm, assigned to the quaternary sp^2 carbon of the benzene ring. The peaks at δ = 129.5 and 132 ppm were assigned to the quaternary and C-H atoms on the imidazole rings, respectively. The peak at 135.2 ppm was assigned to the sp^2 C-H carbon of the triethynylbenzene in the polymer.

2.4 Nitric oxide release

NO release experiments were conducted by suspending each of the solids (30 mg in 25 mL) in PBS at room temperature with stirring, and the concentration of the released NO was monitored using a NO-specific probe. The NO release profiles for the six compounds are shown in **Fig. 6,** along with the solution pH, measured before and after the release experiments were concluded, **Fig. 7**.

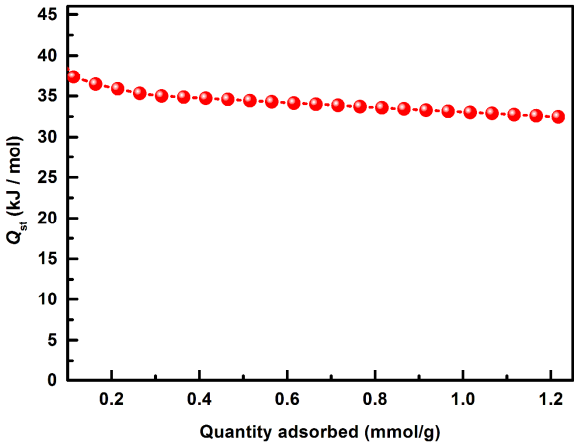

Figure 4. Heat of adsorption (Qst) for NO in TIFSIX-2-Cu-i

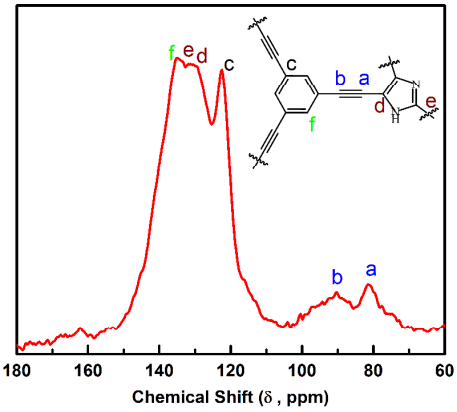

Figure 5. ^{13}C-CPMAS NMR spectrum of imidazole-POP, showing a tentative repeat unit of the polymer with assigned chemical shifts.

Notably, most of the materials studied herein demonstrate rapid release within the first few minutes upon contact with PBS, corresponding to release of weakly adsorbed NO molecules. UiO-66 and UiO-66-NH_2 demonstrated similar release profiles within the first hour, signaling release of physisorbed NO inside both MOFs, **Fig. 6a**. After the rate of release decreased considerably, 0.1 mL of 1 M H_2SO_4 was added to the suspension, upon which a rapid increase in the release of NO was recorded for UiO-66-NH_2, while no detectable increase was observed for UiO-66. This observation demonstrates the role of the free amine functionality within UiO-66-NH_2 to achieve chemisorption of the NO molecules, potentially as *N*-diazeniumdiolates. As UiO-66 contains the same metal-carboxylate clusters as UiO-66-NH_2, the observed enhancement in the total NO uptake (described in the NO sorption section) and the acid-triggered release observed only in the NH_2 variant can be attributed to the presence of the primary amine functionality. NO release from UiO-66-NH_2 continued at a consistent decay rate for about three hours after the acid-triggered release. The pH for the release solution was then measured after the experiment and demonstrated a drop from 7.4 for the PBS to 3, **Fig. 7**, consistent with the high concentration of NO released into solution, where nitric acid is commonly produced as a decomposition product of water-dissolved NO.[48] It is to be noted that simple addition of the 0.1 mL sulfuric acid to the PBS release

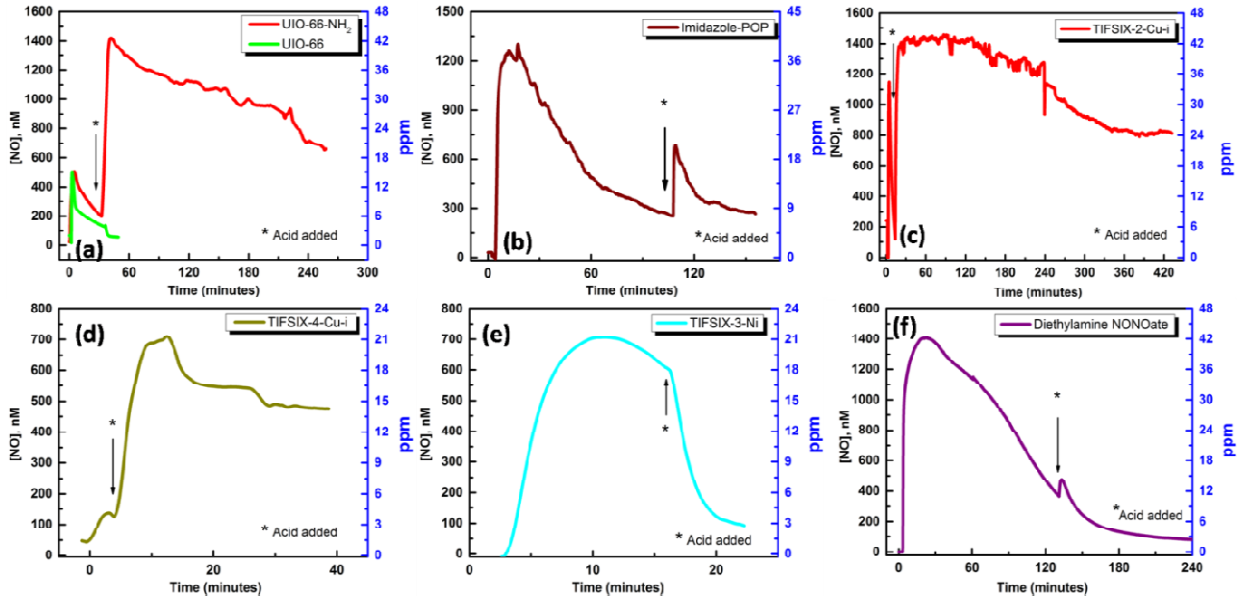

Figure 6. (a-f) Nitric oxide release profiles in PBS (pH = 7.43), and after addition of 0.1 mL of 1M H_2SO_4 to the release media for the reported compounds. Nitric oxide release measured through dispersing 30 mg of the NO-loaded solids in 25 mL of PBS, using NO-specific electrode immersed in the release medium at room temperature.

solution caused a drop of pH from 7.4 to 5.4, **Fig. 7.** The NO release profile for the imidazole-POP is shown in **Fig. 6b**. The release profile reveals rapid release with moderate decay rate within the first hour, reaching 36 ppm of NO. In contrast to the release profile observed in the UiO-66 MOFs, the imidazole-POP initial release peaked at ~ 36 ppm of NO without the need for the acid triggered release, and decayed slowly over the course of 90 minutes. Subsequently, when acid was added, an additional NO release peak was observed, however, this corresponded to a lower quantity of NO when compared to UiO-66-NH_2. This observation can be explained in light of the chemical nature of the imidazole ring, where NO can potentially be covalently anchored to the secondary amine functionality of the imidazole ring. Upon contact with water, it is feasible to assume protonation of the pyridine-like nitrogen of the imidazole ring (pKa 6.9), affecting the chemical stability of the imidazole-nitric oxide compound, and thus triggering the release of NO. In accordance, the observed slight enhancement of NO release upon addition of the acid can be explained in terms of facilitating further protonation of the imidazole rings, effectively releasing the rest of imidazole-bound NO. Indeed, the decrease in pH value of the release medium to pH = 6 upon commencement of the study indicated that the imidazole rings consumed most of the acid, affording displacement of the NO molecules chemisorbed on the POP. The NO release profiles for the three HUMs are presented in **Fig. 6c-e**. In the case of TIFSIX-2-Cu-i, rapid initial release within the first few minutes after mixing can be ascribed to physically adsorbed NO and is similar to that seen for the UiO-MOFs. The rapid decay observed for this initial release can be ascribed to the overall low volume of physisorbed NO within the tight pores of the compound. Interestingly, upon addition of the acid, a rapid increase of NO release was observed, reaching ~ 42 ppm, and decaying slowly over the course of 6 hours. As the material did not show high uptake in the low pressure NO sorption isotherm and demonstrated almost reversible behavior for NO uptake, the observed release

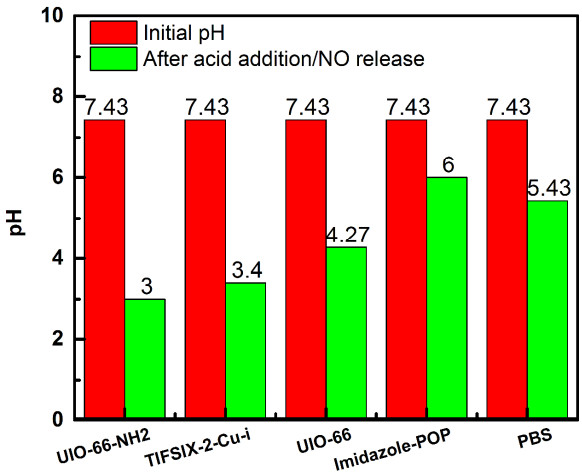

Figure 7. pH changes in the release media

cannot be explained in terms of a physisorption. A possible explanation is that upon high pressure loading of NO, NO molecules are adsorbed within the material through coordination to Cu ions. A recent study utilized electron paramagnetic resonance (EPR) spectroscopy and demonstrated ligand displacement upon NO binding to Ni ions in two examples of MOFs.[49] One way to visualize this process is to assume displacement of the axial TIFSIX species that pillar the square grid structure of the Cu(4,4′-dipyridylacetylene) network, by Cu-coordinated NO molecules. The assumption of displacement of the TIFSIX rather than the pyridyl rings is reasonable considering the weak coordination of TIFSIX to the Cu(II) metal ions through the fluorine atoms and our observations in the context of water sorption.[45] Indeed, unit cell refinement from the PXRD pattern recorded for TIFSIX-2-Cu-i after loading at 10 bar with NO (see **Fig. S6**) indicated retention of tetragonal crystal system (I4/mmm, a= b= 13.674 Å, c = 21.275 Å), but significant change in the c cell

Table 1. Comparison of the performance of NO releasing solids.

Material	Conditions for Release	Amount released	Rate of release	Reference
UiO-66-NH_2	PBS/Acid	1.1 mmol/g*	Initial burst followed by delayed, acid-catalyzed release ~ 4 hours	This work *maximum released
TIFSIX-2-Cu-i	PBS/Acid	1.2 mmol/g*	Initial burst followed by delayed, acid-catalyzed release ~ 7 hours	This work
Imidazole-POP	PBS/Acid	1.04 mmol/g *	Initial release within 1 hour followed by delayed, acid-catalyzed release ~ 3 hours	This work
TIFSIX-4-Cu-i	PBS/Acid	0.6 mmol/g *	Initial low release followed by delayed, acid-catalyzed release ~ 1 hour	This work
TIFSIX-3-Ni	PBS/Acid	0.6 mmol/g*	Spontaneous release within 30 minutes, no effect of the acid	This work
Fe_2(dobdc)	11% relative humidity in N_2 at 310 K	4 mmol/g	Still evolving after 10 days (ppb levels)	50
Ni_2(dobdc)	11% relative humidity	6.7 mmol/g	Initially with flowing wet gas, half life of NO deliv-ery reduced from several hours (in wet gas) to ~10 minute when in contact with PBS)	23
Co_2(dobdc)	11% relative humidity	7.0 mmol/g	Most NO released after 5 h	23
Mg_2(dobdc)	11% relative humidity	0.1 molecules per unit cell, 2% of stored capacity	Negligible quantity released	22
Mg_2(dobdc) Ni doped (40%)	11% relative humidity	14 molecules per unit cell	Up to 45 hours (to 20 ppb), 82% release of stored NO	22
Zn_2(dobdc)	11% relative humidity	0.3 molecules per unit cell	Primarily released within first 2-3 hours	22
Zn_2(dobdc) Ni doped (>10%)	11% relative humidity	2.4 molecules per unit cell	Primarily released within first 1.5 hours	22
MIL-100(Fe)	11% relative humidity, 200 mL/min	0.55 mmol/g	Primarily released in first 2.5 hours continues up to 25 h	46
MIL-100(Cr)	11% relative humidity, 200 mL/min	0.65 mmol/g	26% NO released, primarily released in first 2.5 hours but continues up to 40 h	46
MIL-127(Fe)	11% relative humidity, 200 mL/min	0.49 mmol/g	36% NO released, primarily released in first 5 hours continues up to 20 h	46
CuBTTri (acting upon *S*-nitrosocysteamine as a catalyst)	PBS, 298 K	N/A	Rate of release 22.8 nM/s	51
NOF-11 (with bis-*N*-nitroso) moiety (modification of MIL-125)	Light irradiation (300 W xenon lamp, 300-600 nm)	1.0 mmol/g	3600 s	52
NOF-12 (with bis-*N*-nitroso) moiety (modification of CAU-1)	Light irradiation (300 W xenon lamp, 300-600 nm)	1.4 mmol/g	3600 s	52
MIL-88	11% relative humidity, 200 mL/min, 303 K	0.14 mmol/g	Most NO released in 1 h, but continues to 16 h	53
IRMOF-3-NONO	Griess assay, aqueous media (phosphate buffer)	0.51 mmol/g	8% of amine sites releasing NO in IRMOF-3-NONO, almost immediate	54
UMCM-1-NONO	Griess assay	0.10 mmol/g	6% of amine sites releasing NO in UMCM-1-NONO, almost immediate	54
UHM-36	11% relative humidity	0.0157 mmol/g	7.02 half life period/min, 2 h for release	21
UHM-37	11% relative humidity	0.0644mmol/g	64.45 half life period/min, 6 h for release	21
UHM-38	11% relative humidity	0.0262mmol/g	26.21 half life period/min, 3 h for release	21
UHM-39	11% relative humidity	0.0225mmol/g	22.54 half life period/min, 7 h for release	21
HKUST-1	11% relative humidity	0.001 mmol/g	Nearly complete after 20 min, continues for up to 60 min	44
Natural Zeolite	PBS (37°C, pH 7.4)	0.17-0.33 mmol/g	Most released in the first 60 min, gradual increase after 180 min	55
	Deionized water	0.22 mmol/g	Most released within 240 min, no further change in nitrite concentration after that	55
Cu-MCM-41	3-Morpholino-2 hydroxy-propane sulfonic acid buffer	0.0086 mmol/g	Complete release within 60 min	56
Cu-TDPAT (diazeniumdiolated MOF)	85% relative humidity, room temperature	0.175 mmol/g after 7 days	Initial burst in the first 3 hrs, then continued slower release	57
Electrospun fibres of AN/VIM/IP terpolymer	85% relative humidity, 37°C	0.068 mmol/g over 7 days	Steady release for 14 days	58
Electrospun fibres of AN/VIM/BA terpolymer	85% relative humidity, 37°C	0.062 mmol/g over 7 days, 0.079 mmol/g over 14 days	Steady release for 14 days	58

parameter vs. TIFSIX-2-Cu-i (I4/mmm, a = b= 13.6955(5) Å, c = 8.1724(4) Å). The expansion along the c-axis, the axis parallel to the inorganic TiF_6^{2-} pillars, can be explained by assuming that Cu-NO coordination occurs forcing the square grid (**sql**) layers to separate in a clay-like fashion. Water molecules serve to cause such as effect in SIFSIX-3-Ni.[45] This phase change could explain the poorly crystalline PXRD observed, and contribute to the loss of intensity of the 110 and 200 peaks (2θ = 9.132°and 12.923°) in the PXRD of the NO-loaded TIFSIX-2-Cu-i (see SI for further details). The observed enhancement of NO release upon acid addition can then be explained as the result of decomposing the material by protonation of the pyridine-containing linkers, thus changing the overall coordination environment of the Cu ions and resulting in the loss of NO coordination. The pH of the release

medium was found to be 3.4 which reflects the high concentration of NO released to the medium. When the precipitated solid was isolated from the release medium, dried, and analyzed through XRD, the obtained diffraction pattern did not resemble the starting material, but rather indicated an amorphous solid, supporting framework degradation. TIFSIX-4-Cu-i is isoreticular to TIFSIX-2-Cu-i but its square grid dimensions are expanded as a result of its expanded linker, 1,4-di(pyridine-4-yl)benzene vs. 4,4′-dipyridylacetylene. As a consequence of its chemical composition, the density of the Cu ions (the active binding sites for NO) within this HUM is lower than that in TIFSIX-2-Cu-i. The NO release profile shown in **Fig.6d** for TIFSIX-4-Cu-i demonstrated that the initial rapid release of NO was followed by additional NO release of up to 21 ppm after addition of the acid. This observation is in further agreement with the hypothesis that Cu-NO coordination contributes to the relatively large uptake and release of NO within the investigated HUMs. Interestingly, when NO release was investigated for TIFSIX-3-Ni, rapid release to a level of 21 ppm was observed, but adding acid had no noticeable effect in triggering further release of NO, **Fig.6e.** This HUM exhibited lower release of NO when compared to TIFSIX-2-Cu-i and TIFSIX-4-Cu-i. A possible explanation for this trend is the weaker ability of Ni ions to coordinate NO molecules compared to Cu ions. This is in agreement with commonly observed trends of Cu(II) vs. Ni(II) coordination compounds, where Cu(II) octahedral complexes are more frequently observed especially in MX_4Y_2 configuration, where X and Y are coordination ligands of different nature. For comparison, we also carried out NO release from diethylamine NONOate, **Fig. 6f**. Interestingly at a dose of 1 mg per 25 mL of the PBS release solution, the NONOate exhibited NO release reaching a maximum of 42 ppm within 30 minutes of contact with the release medium followed by rapid decay. The NO concentration within the release medium decayed almost to the background level within 4 hours. In comparison to the three most promising NO releasing solids described earlier, UiO-66-NH_2/ imidazole-POP/ TIFSIX-2-Cu-i the benefit of storing NO within microporous solids becomes evident: slow release of NO reaching almost the same initial release from the diethylamine NONOate, but the much larger acid-triggered release was not observed in case of the molecular NONOate.

Our results, are compared to those found in the literature, as shown in **Table 1**, and indicate that some of the materials investigated herein offer release profiles that afford up to 1.2 mmol of NO per gram of material over a period of up to seven hours. While the material investigated here demonstrated the second largest release of NO, after MOFs having open metal sites reported by Morris and co-workers, [23] our material demonstrated the acid-triggered response for NO release, in contrast to the spontaneous release upon contact with moisture commonly observed for some of the best NO storing MOFs. The release profiles are also of note as being the first to demonstrate acid-triggered release of NO in PBS, paving the way for controlled release of NO from microporous solids that are safe to transport and handle, either through acid trigger or other chemical/physical NO-release trigger.

3. Conclusion

Three different classes of microporous solids that exhibit a variety of building units, chemical functionality, pore systems, and available binding sites were investigated as potential candidates for efficient NO storage and release. Strong chemisorption of NO inside the highly porous, amine functionalized UiO-66-NH_2 can be ascribed to the presence of amine functionality, in contrast to the prototypal UiO-66. The HUMs family demonstrated metal ion-specific binding behavior of NO, wherein Cu ions exhibit better affinity for NO uptake than Ni ions. In addition, as the HUMs investigated herein did not show high uptake in the low pressure NO sorption study, and rather demonstrated almost reversible behavior for NO uptake up to ~ 1bar, the observed release cannot be explained in terms of physisorption. Rather, it is possible that high pressure loading of NO leads to chemisorption as coordination complexes, most likely through axial coordination displacing the pillaring TiF_6 anions. The imidazole-POP material demonstrated spontaneous release of NO upon contact with the release medium without acid to trigger the release. The systematic study of three different types of solids, MOFs, POPs and HUMs, presented herein demonstrates important structure-property relationships that may be applied to the tailored design of materials for the controlled delivery of NO.

4. Experimental Procedure:

All chemicals and reagents were of commercial grade used as received without further purification. For more detailed experimental conditions and procedure please see the SI.

Loading with nitric oxide: The solids were placed in closed Eppendorf tubes with the caps punctured with a needle to allow for efficient gas exchange. Loading with nitric oxide was conducted in a stainless steel pressure reactor (BuchiGlasuster miniclave steel) fitted with Teflon insert and pressure gauge. The system was flushed with nitrogen then pressurized with 10 bar of NO (BOC, AK 35 bar Nitric Oxide N2.5) at room temperature for 12 hours. After the loading was complete, the NO pressure was released gradually in a fumehood; the reactor was then flushed with 10 bar of nitrogen briefly, then opened to air and the material transferred into a desiccator for the NO release study.

Caution: NO is a toxic gas. All work with NO gas was conducted inside a properly ventilated fumehood. A BW GasAlert NO gas sensor for NO was also used to monitor the levels of NO during the experiment.

Nitric oxide release study: The release study was conducted with an (inNOII) nitric oxide detection system (Innovative instruments, Inc.) equipped with (amiNO-700) electrodes in phosphate buffer saline (PBS, pH of 7.4) at room temperature. In a typical experiment, 30 mg of solid was suspended in 25 mL of the PBS buffer in falcon tubes with a magnetic stirrer. The exception was for diethylamine NONOate where only 1mg was added to 25 mL of PBS solution. The levels of NO released were monitored *via* the NO-specific electrodes (amiNO-700) where the electrodes were calibrated prior to use according to the manufacturer's specifications. Diethylamine NONOate sodium salt hydrate, was purchased from Sigma-Aldrich and used as received.

Associated Content

Supporting Information

The Supporting Information is available free of charge on the ACS Publications website at DOI:

Experimental Procedures, FT-IR, NO sorption, and crystallographic data.

Author Information

Corresponding Authors

*E-mail: michael.zaworotko@ul.ie

*E-mail: m.yacoub@imperial.ac.uk

*E-mail: malkordi@mail.usf.edu

Notes

The authors declare no competing financial interest.

Acknowledgement

We acknowledge funding from Harefield NHS Foundation Trust, Imperial College-London, the Magdi Yacoub Institute, Zewail City of Science and Technology, University of Limerick, and Science Foundation Ireland (SFI award 13/RP/B2549).

References

1. Moncada, S.; Palmer, R. M.; Higgs, E. A., *Pharmacol Rev* **1991,** 43 (2), 109-142.
2. Forstermann, U.; Munzel, T., *Circulation* **2006,** 113 (13), 1708-1714.
3. Tonelli, A. R.; Haserodt, S.; Aytekin, M.; Dweik, R. A., *Pulm Circ* **2013,** 3 (1), 20-30.
4. Wimalawansa, S. J., *Expert Opin Pharmacother* **2008,** 9 (11), 1935-1954.
5. Riccio, D. A.; Schoenfisch, M. H., *Chem. Soc. Rev.* **2012,** 41 (10), 3731-3741.
6. Lam, C. F.; Sviri, S.; Ilett, K. F.; van Heerden, P. V., *Expert Opin Investig Drugs* **2002,** 11 (7), 897-909.
7. Liu, J.; Li, C.; Qu, W.; Leslie, E.; Bonifant, C. L.; Buzard, G. S.; Saavedra, J. E.; Keefer, L. K.; Waalkes, M. P., *Mol Cancer Ther* **2004,** 3 (6), 709-714.
8. Nablo, B. J.; Rothrock, A. R.; Schoenfisch, M. H., *Biomaterials* **2005,** 26 (8), 917-924.
9. Konter, J.; Abuo-Rahma, G. E.-D. A. A.; El-Emam, A.; Lehmann, J., *Eur. J. Org. Chem.* **2007,** 2007 (4), 616-624.
10. Wheatley, P. S.; Butler, A. R.; Crane, M. S.; Fox, S.; Xiao, B.; Rossi, A. G.; Megson, I. L.; Morris, R. E., *J. Am. Chem. Soc.* **2006,** 128 (2), 502-509.
11. McKinlay, A. C.; Morris, R. E.; Horcajada, P.; Ferey, G.; Gref, R.; Couvreur, P.; Serre, C., *Angew. Chem. Int. Ed. Engl.* **2010,** 49 (36), 6260-6266.
12. Parzuchowski, P. G.; Frost, M. C.; Meyerhoff, M. E., *J. Am. Chem. Soc.* **2002,** 124 (41), 12182-12191.
13. Reynolds, M. M.; Hrabie, J. A.; Oh, B. K.; Politis, J. K.; Citro, M. L.; Keefer, L. K.; Meyerhoff, M. E., *Biomacromolecules* **2006,** 7 (3), 987-994.
14. Zhang, H.; Annich, G. M.; Miskulin, J.; Stankiewicz, K.; Osterholzer, K.; Merz, S. I.; Bartlett, R. H.; Meyerhoff, M. E., *J. Am. Chem. Soc.* **2003,** 125 (17), 5015-5024.
15. Shin, J. H.; Metzger, S. K.; Schoenfisch, M. H., *J. Am. Chem. Soc.* **2007,** 129 (15), 4612-4619.
16. AbdulHalim, R. G.; Shkurenko, A.; Alkordi, M. H.; Eddaoudi, M., *Crystal Growth & Design* **2016,** 16 (2), 722-727.
17. Chen, K.-J.; Scott, Hayley S.; Madden, David G.; Pham, T.; Kumar, A.; Bajpai, A.; Lusi, M.; Forrest, Katherine A.; Space, B.; Perry, John J.; Zaworotko, Michael J., *Chem* **2016,** 1 (5), 753-765.
18. Rapti, S.; Pournara, A.; Sarma, D.; Papadas, I. T.; Armatas, G. S.; Hassan, Y. S.; Alkordi, M. H.; Kanatzidis, M. G.; Manos, M. J., *Inorg. Chem. Front.* **2016,** 3 (5), 635-644.
19. Luebke, R.; Belmabkhout, Y.; Weseliński, Ł. J.; Cairns, A. J.; Alkordi, M.; Norton, G.; Wojtas, Ł.; Adil, K.; Eddaoudi, M., *Chemical Science* **2015,** 6 (7), 4095-4102.
20. Alkordi, M. H.; Eddaoudi, M. In *Supramol. Chem.*, John Wiley & Sons, Ltd: 2012.
21. Peikert, K.; McCormick, L. J.; Cattaneo, D.; Duncan, M. J.; Hoffmann, F.; Khan, A. H.; Bertmer, M.; Morris, R. E.; Fröba, M., *Microporous Mesoporous Mater.* **2015,** 216, 118-126.
22. Cattaneo, D.; Warrender, S. J.; Duncan, M. J.; Kelsall, C. J.; Doherty, M. K.; Whitfield, P. D.; Megson, I. L.; Morris, R. E., *RSC Adv* **2016,** 6 (17), 14059-14067.
23. McKinlay, A. C.; Xiao, B.; Wragg, D. S.; Wheatley, P. S.; Megson, I. L.; Morris, R. E., *J. Am. Chem. Soc.* **2008,** 130 (31), 10440-10444.
24. Nugent, P.; Belmabkhout, Y.; Burd, S. D.; Cairns, A. J.; Luebke, R.; Forrest, K.; Pham, T.; Ma, S.; Space, B.; Wojtas, L.; Eddaoudi, M.; Zaworotko, M. J., *Nature* **2013,** 495 (7439), 80-84.
25. Shekhah, O.; Belmabkhout, Y.; Chen, Z.; Guillerm, V.; Cairns, A.; Adil, K.; Eddaoudi, M., *Nat Commun* **2014,** 5, 4228.
26. Cui, X.; Chen, K.; Xing, H.; Yang, Q.; Krishna, R.; Bao, Z.; Wu, H.; Zhou, W.; Dong, X.; Han, Y.; Li, B.; Ren, Q.; Zaworotko, M. J.; Chen, B., *Science* **2016,** 353 (6295), 141-144.
27. Chen, K. J.; Madden, D. G.; Pham, T.; Forrest, K. A.; Kumar, A.; Yang, Q. Y.; Xue, W.; Space, B.; Perry, J. J. t.; Zhang, J. P.; Chen, X. M.; Zaworotko, M. J., *Angew. Chem. Int. Ed. Engl.* **2016,** 55 (35), 10268-10272.
28. Kumar, A.; Madden, D. G.; Lusi, M.; Chen, K. J.; Daniels, E. A.; Curtin, T.; Perry, J. J. t.; Zaworotko, M. J., *Angew. Chem. Int. Ed. Engl.* **2015,** 54 (48), 14372-14377.
29. Haikal, R. R.; Wang, X.; Hassan, Y. S.; Parida, M. R.; Murali, B.; Mohammed, O. F.; Pellechia, P. J.; Fontecave, M.; Alkordi, M. H., *ACS Appl. Mater. Interfaces* **2016,** 8 (31), 19994-20002.
30. Soliman, A. B.; Haikal, R. R.; Hassan, Y. S.; Alkordi, M. H., *Chem. Commun.* **2016,** 52, 12032-12035.
31. Alkordi, M. H.; Haikal, R. R.; Hassan, Y. S.; Emwas, A.-H.; Belmabkhout, Y., *J. Mater. Chem. A* **2015,** 3 (45), 22584-22590.
32. Sofia Rapti, A. P., Debajit Sarma, Ioannis T. Papadas, Gerasimos S. Armatas, Youssef S. Hassan, Mohamed H. Alkordi, Mercouri G. Kanatzidisb; Manos, M. J., *Inorg. Chem. Front.* **2016,** 3, 635-644.
33. Wood, C. D.; Tan, B.; Trewin, A.; Su, F.; Rosseinsky, M. J.; Bradshaw, D.; Sun, Y.; Zhou, L.; Cooper, A. I., *Adv. Mater.* **2008,** 20 (10), 1916-1921.
34. Dawson, R.; Cooper, A. I.; Adams, D. J., *Prog. Polym. Sci.* **2012,** 37 (4), 530-563.
35. Cavka, J. H.; Jakobsen, S.; Olsbye, U.; Guillou, N.; Lamberti, C.; Bordiga, S.; Lillerud, K. P., *J. Am. Chem. Soc.* **2008,** 130 (42), 13850-13851.
36. Morris, W.; Volosskiy, B.; Demir, S.; Gandara, F.; McGrier, P. L.; Furukawa, H.; Cascio, D.; Stoddart, J. F.; Yaghi, O. M., *Inorg. Chem.* **2012,** 51 (12), 6443-6445.
37. Haikal, R. R.; Elmansi, A. M.; Ali, P.; Hassan, Y. S.; Alkordi, M. H., *RSC Adv.* **2016,** 6 (48), 42307-42312.

38. Kandiah, M.; Nilsen, M. H.; Usseglio, S.; Jakobsen, S.; Olsbye, U.; Tilset, M.; Larabi, C.; Quadrelli, E. A.; Bonino, F.; Lillerud, K. P., *Chem. Mater.* **2010,** 22 (24), 6632-6640.
39. Kumar, A.; Hua, C.; Madden, D. G.; O'Nolan, D.; Chen, K. J.; Keane, L. J.; Perry, J. J.; Zaworotko, M. J., *Chem Commun (Camb)* **2017,** 53 (44), 5946-5949.
40. Wu, D.; Xu, F.; Sun, B.; Fu, R.; He, H.; Matyjaszewski, K., *Chem. Rev.* **2012,** 112 (7), 3959-4015.
41. Karabacak, M.; Cinar, M.; Unal, Z.; Kurt, M., *J. Mol. Struct.* **2010,** 982 (1–3), 22-27.
42. Lee, J.; Farha, O. K.; Roberts, J.; Scheidt, K. A.; Nguyen, S. T.; Hupp, J. T., *Chem. Soc. Rev.* **2009,** 38 (5), 1450-1459.
43. Bloch, E. D.; Queen, W. L.; Chavan, S.; Wheatley, P. S.; Zadrozny, J. M.; Morris, R.; Brown, C. M.; Lamberti, C.; Bordiga, S.; Long, J. R., *J. Am. Chem. Soc.* **2015,** 137 (10), 3466-3469.
44. Xiao, B.; Wheatley, P. S.; Zhao, X.; Fletcher, A. J.; Fox, S.; Rossi, A. G.; Megson, I. L.; Bordiga, S.; Regli, L.; Thomas, K. M.; Morris, R. E., *J. Am. Chem. Soc.* **2007,** 129 (5), 1203-1209.
45. O'Nolan, D.; Kumar, A.; Zaworotko, M. J., *J. Am. Chem. Soc.* **2017,** 139 (25), 8508-8513.
46. Eubank, J. F.; Wheatley, P. S.; Lebars, G.; McKinlay, A. C.; Leclerc, H.; Horcajada, P.; Daturi, M.; Vimont, A.; Morris, R. E.; Serre, C., *APL Mater.* **2014,** 2 (12), 124112.
47. Bonino, F.; Chavan, S.; Vitillo, J. G.; Groppo, E.; Agostini, G.; Lamberti, C.; Dietzel, P. D. C.; Prestipino, C.; Bordiga, S., *Chem. Mater.* **2008,** 20 (15), 4957-4968.
48. Armor, J. N., *Journal of Chemical & Engineering Data* **1974,** 19 (1), 82-84.
49. Mendt, M.; Gutt, F.; Kavoosi, N.; Bon, V.; Senkovska, I.; Kaskel, S.; Pöppl, A., *J. Phys. Chem. C* **2016,** 120 (26), 14246-14259.
50. Barth, B.; Mendt, M.; Pöppl, A.; Hartmann, M., *Microporous Mesoporous Mater.* **2015,** 216, 97-110.
51. Harding, J. L.; Metz, J. M.; Reynolds, M. M., *Adv. Funct. Mater.* **2014,** 24 (47), 7503-7509.
52. Kim, C.; Diring, S.; Furukawa, S.; Kitagawa, S., *Dalton Transactions* **2015,** 44 (34), 15324-15333.
53. McKinlay, A. C.; Eubank, J. F.; Wuttke, S.; Xiao, B.; Wheatley, P. S.; Bazin, P.; Lavalley, J. C.; Daturi, M.; Vimont, A.; De Weireld, G.; Horcajada, P.; Serre, C.; Morris, R. E., *Chem. Mater.* **2013,** 25 (9), 1592-1599.
54. Nguyen, J. G.; Tanabe, K. K.; Cohen, S. M., *CrystEngComm* **2010,** 12 (8), 2335-2338.
55. Narin, G.; Albayrak, Ç. B.; Ülkü, S., *Applied Clay Science* **2010,** 50 (4), 560-568.
56. Boës, A.-K.; Xiao, B.; Megson, I. L.; Morris, R. E., *Top. Catal.* **2008,** 52 (1-2), 35-41.
57. Lowe, A.; Chittajallu, P.; Gong, Q.; Li, J.; Balkus, K. J., *Microporous Mesoporous Mater.* **2013,** 181, 17-22.
58. Lowe, A.; Bills, J.; Verma, R.; Lavery, L.; Davis, K.; Balkus, K. J., Jr., *Acta Biomater* **2015,** 13, 121-30.

TOC Graphic